# Stable Overlapping Replicator Dynamics for Subnetwork Identification

**Bernard Ng**[1,2], **Burak Yoldemir**[3], **Rafeef Abugharbieh**[3]

[1]Parietal team, Neurospin, INRIA Saclay, France
[2]FIND Lab, Stanford University, United States
[3]Biomedical Signal and Image Computing Lab, University of British Columbia, Canada
*bernardyng@gmail.com, yoldemir@gmail.com, rafeef@ece.ubc.ca*

## Abstract

Recent years witnessed an emerging interest in studying brain dynamics using functional magnetic resonance imaging (fMRI). For brain regions to interact with different parts of the brain at different times, the underlying subnetworks must necessarily overlap. Recently, many overlapping community detection techniques are put forth in response to the rapidly growing demand for these tools in network analysis applications. However, few of these techniques consider the critical need to statistically control for false node inclusion in the detected network communities. In this paper, we propose a novel technique for identifying overlapping subnetworks from weighted graphs that controls for false node inclusion. Our technique builds upon the overlapping replicator dynamics (ORD) formulation but additionally exploits a graph incrementation scheme to enable merging of subnetwork components that are falsely split by ORD due to its stringent mutual similarity criterion for grouping nodes. Further, we present a procedure for integrating stability selection into ORD so that false node inclusion arising from noise and over-merging are statistically controlled. We refer to our technique as stable ORD (SORD). Validating on synthetic data, we show a significant increase in subnetwork identification accuracy compared to state-of-the-art techniques. Moreover, superior test-retest reliability is demonstrated on the Human Connectome Project (HCP) data, with neuroanatomically-meaningful subnetworks and brain hubs identified.

## 1 Introduction

Analyzing the brain by grouping interacting regions into subnetworks provides enormous insight into the brain's organizational structure. One of the dominant tools facilitating such analysis is functional magnetic resonance imaging (fMRI). The most common techniques for extracting subnetworks from fMRI data include seed-based analysis and spatial independent component analysis (ICA) [1]. Recently, the graph theoretic approach that models brain regions as graph nodes and the strength of their interactions through edge weights has gained popularity due to advances in graph community detection methods [2]. Graph partitioning techniques, such as normalized cut [3], Louvain [2], and the modularity maximization algorithm [2], are widely used but are limited to grouping nodes into disjoint subnetworks, which does not capture how certain brain regions are known to interact with different parts of the brain at different times. For such interactions to occur, the underlying subnetworks must necessarily overlap. Devising methods that permit identification of overlapping subnetworks is thus crucial for a more accurate understanding of the brain's organization.

To identify overlapping subnetworks in the brain, a number of techniques have been

explored. Wu et al. proposed clustering nodes into maximal cliques on which graph partitioning is performed, followed by regrouping of nodes into overlapping subnetworks based on their partition assignment [4]. The drawback of this technique is that the identified subnetworks are sensitive to parameters, such as the number of subnetworks to extract and the minimum clique size. Yan et al. adopted a technique called connected iterative scan (CIS), which iteratively determines whether each node of a graph belongs to a given subnetwork based on its influence on a density metric when added to that subnetwork [5]. CIS is very simple to implement, but the extracted subnetworks are sensitive to the weighting factor used for controlling subnetwork size. Smith et al. proposed using temporal ICA to compensate for the lack of subnetwork overlaps with spatial ICA due to its spatial independence criterion, but the proposed implementation uses an ad hoc threshold for extracting interacting nodes from the spatial maps [6]. Recently, we proposed an technique called overlapping replicator dynamics (ORD) that uses mutual similarity between nodes for identifying overlapping subnetworks on weighted graphs [7]. The advantage of ORD is that it has an intrinsic criterion for determining the number of subnetworks in a data-driven manner. Also, ORD removes the need for thresholding in contrast to ICA, as ascribed to its equivalence to non-negative sparse principal component analysis (PCA) [8] with the level of sparsity implicitly selected based on mutual similarity. However, mutual similarity is a very stringent criterion, which tends to falsely split the subnetworks [9]. For a general review of overlapping community detection techniques, we refer readers to [10].

A serious limitation in most community detection techniques is their sole focus on optimizing a criterion, such as modularity, without considering if the optimal communities extracted are statistically significant. This general concern is receiving great attention from the statistics community especially in the area of high dimensional modeling [11-13]. For instance, optimizing the least absolute shrinkage and selection operator (LASSO) objective will provide an optimal sparse solution, but many selected variables might pertain to noise. To control for false detections, techniques for computing p-values in high dimensional settings are under active investigation [11,13], and we argue here that statistical control should similarly be exerted in community detection problems. A notable exception is the Order Statistics Local Optimization Method (OSLOM) [14], which uses a statistical criterion based on a null model derived from random graphs for assessing the significance of the identified subnetworks, and is shown to outperform many state-of-the-art techniques [14].

In this paper, we propose a novel subnetwork identification technique that 1) can operate on weighted graphs, 2) allows for subnetwork overlaps, 3) has an implicit criterion for setting the number of subnetworks, 4) does not force all nodes to be assigned to a subnetwork, and 5) provides statistical control over false node inclusion in the detected subnetworks. Our technique builds upon the ORD formulation but additionally exploits a graph incrementation scheme to facilitate merging of subnetwork components that are falsely split by ORD due to its strict mutual similarity criterion. However, this scheme involves setting a parameter that governs the sparsity level of the identified subnetworks. If set incorrectly, over-merging might occur, which would result in inclusion of false nodes in addition to those arising from noise. To jointly resolve these problems, we propose integrating stability selection [12] into the ORD formulation. The underlying idea is to declare a node as part of a subnetwork only if its probability of being selected over subsamples/bootstraps for various sparsity levels is higher than a theoretical threshold that provably controls the expected number of false nodes included. The basis of stability selection is that consistently selecting the same false nodes over a large number of bootstraps is statistically unlikely. Importantly, stability selection is insensitive to the choice of sparsity levels. Thus, incorporating stability selection enables removal of false nodes arising from noise and over-merging in a data-driven fashion. Integrating stability selection into subnetwork identification is generally nontrivial due to the need for establishing subnetwork correspondence across bootstraps. This problem is especially challenging when the subnetworks are allowed to overlap and are estimated from noisy graphs. We resolve this problem by exploiting an intrinsic property of RD, namely the initialization of the RD process governs the subnetwork to which RD converges to. We refer to our proposed technique as stable overlapping replicator dynamics (SORD). To evaluate SORD, we compare it against a number of state-of-the-art techniques on synthetic data comprising a wide array of network configurations as well as assess its test-retest reliability on the Human Connectome Project (HCP) data [15].

# 2 Methods

We first review the properties of RD (Section 2.1) that enable overlapping subnetwork identification (Section 2.2). We then describe a graph incrementation scheme for merging subnetwork components that might be falsely split by ORD and how stability selection can be integrated to statistically control for false node inclusion (Section 2.3).

## 2.1 Replicator Dynamics

Let $\mathbf{C}$ be a $d \times d$ weighted adjacency matrix. Replicator dynamics can be shown to maximize the following non-convex optimization problem [8]:

$$\max_{\mathbf{w}} \mathbf{w}^T \mathbf{C} \mathbf{w} \quad s.t. \left\| \mathbf{w} \right\|_1 = 1, \mathbf{w} \geq 0, \tag{1}$$

which is a simple variant of non-negative sparse PCA, where non-zero values in $\mathbf{w}$ indicate the corresponding nodes belong to the same subnetwork. This non-convex problem (1) comprises multiple local maxima that can be found by iterating [16]:

$$\mathbf{w}(k+1) = \frac{\mathbf{w}(k) .* \mathbf{C}\mathbf{w}(k)}{\mathbf{w}(k)^T \mathbf{C}\mathbf{w}(k)}, \tag{2}$$

where .* denotes element-wise multiplication and $k$ is the iteration number. Based on the fundamental theorem of natural selection, if $\mathbf{C}$ is real, symmetric, and non-negative, $\mathbf{w}(k)^T\mathbf{C}\mathbf{w}(k)$ will strictly increase with increasing $k$ until it converges to a strict local maximum of $\mathbf{w}^T\mathbf{C}\mathbf{w}$ [16]. Denoting the $j^{\text{th}}$ element of $\mathbf{C}\mathbf{w}(k)$ as $(\mathbf{C}\mathbf{w}(k))_j$, which corresponds to the weighted average similarity between node $j$ and other nodes in the identified subnetwork, since $\mathbf{w}_j(k+1) = \mathbf{w}_j(k)$ upon convergence of (2), $(\mathbf{C}\mathbf{w}(k))_j = \mathbf{w}(k)^T\mathbf{C}\mathbf{w}(k)$ for all $j$. Thus, RD is grouping nodes based on mutual similarity. The local maximum at which RD converges highly depends on $\mathbf{w}(0)$. Since the vicinity at which the local maxima reside is not known a priori, an unbiased way of setting $\mathbf{w}(0)$ is to assign all elements of $\mathbf{w}(0)$ to $1/d$, which tends to extract the subnetwork with the highest mutual similarity between nodes [8]. Other local maxima can be found using ORD (Section 2.2). In the present context of identifying subnetworks from fMRI data, each element of $\mathbf{C}$, denoted as $\mathbf{C}_{ij}$, corresponds to the functional connectivity between brain regions of interest (ROIs) $i$ and $j$. We estimate $\mathbf{C}_{ij}$ using Pearson's correlation between ROI time courses. To make $\mathbf{C}$ non-negative so that the properties of RD hold, we set the negative elements of $\mathbf{C}$ to zero due to the currently unclear interpretation of negative correlations. If large negative correlations correspond to signal, we can apply RD to the absolute value of $\mathbf{C}$. Conversely, if large negative correlations correspond to noise, we can apply RD to $\mathbf{C} - \min_{i \neq j}\{\mathbf{C}_{ij}\}$. Also, we set $\mathbf{C}_{ii}$ to 0 since Pearson's correlation does not provide estimates of self connections.

## 2.2 Overlapping Replicator Dynamics

Let $\mathbf{w}_{S1}$ be the first solution found by applying RD on $\mathbf{C}$ and $S_1$ be the set of nodes in the detected subnetwork. One way to find other subnetworks is to destabilize $\mathbf{w}_{S1}$ as a solution of (1) so that RD will converge to another local maximum. This can be achieved by augmenting $\mathbf{C}$ as follows [17]:

$$\mathbf{C}_{ij}^{aug} = \begin{cases} \mathbf{C}_{ij} & \text{if } i, j \leq d \\ \alpha & \text{if } j > d \text{ and } i \notin S_{j-d} \\ \beta & \text{if } i, j > d \text{ and } i = j \\ \gamma_{ij} & \text{if } i > d \text{ and } j \in S_{i-d} \\ 0 & \text{otherwise} \end{cases} \tag{3}$$

$$\gamma_{ij} > \frac{1}{|S_{i-d}|} \sum_{m \in S_{i-d}} \mathbf{C}_{mj} \tag{4}$$

where $\alpha > \beta$, $\beta = \max_{i \neq j} \mathbf{C}_{ij}$, and $|\cdot|$ denotes cardinality. In effect, this is equivalent to adding an artificial node to the graph by appending $\mathbf{C}$ with a new row and a new column, and extending weighted edges to the original nodes such that $\mathbf{w}_{S1}$ provably becomes unstable [17]. $S_2$ can be found by setting elements of $\mathbf{w}(0)$ to $1/d$ and applying (2) to $\mathbf{C}^{aug}$, with convergence to a local maximum guaranteed despite $\mathbf{C}^{aug}$ being asymmetric [17]. Other subnetworks can be similarly extracted. We highlight that a natural criterion for terminating further subnetwork extraction would be to stop if $\mathbf{w}(k)^{\mathrm{T}}\mathbf{C}\mathbf{w}(k)$ after convergence is less than or equal to $\mathbf{w}(0)^{\mathrm{T}}\mathbf{C}\mathbf{w}(0)$, since this suggests that no further solutions of (1) are present. In practice, we empirically found on synthetic data encompassing a wide assortment of network configurations (Section 3) that $\mathbf{w}(k)^{\mathrm{T}}\mathbf{C}\mathbf{w}(k) \leq 5 \cdot \mathbf{w}(0)^{\mathrm{T}}\mathbf{C}\mathbf{w}(0)$ is more robust to noisy $\mathbf{C}$. Note that we generated an independent set of synthetic data that is separate from the synthetic data used for method comparisons in setting this termination parameter.

## 2.3 Stable Overlapping Replicator Dynamics

**Graph incrementation.** With mutual similarity as the criterion for grouping nodes, applying ORD on a noisy $\mathbf{C}$ could easily result in a subnetwork being falsely split into components [9], since even small perturbations to $\mathbf{C}$ would render certain nodes non-mutually connected. To reduce this effect, one strategy is to add a constant, $\eta$, to the off diagonal elements of $\mathbf{C}$. Using an extreme example for intuition, if we add 10,000 to a $\mathbf{C}$ with values ranging from 0 to 1, the original differences between elements of $\mathbf{C}$ would be negligible. Applying RD to such a $\mathbf{C}$ would result in all nodes assigned to a single subnetwork, i.e. non-zero values for all elements of $\mathbf{w}$. If we instead use a $\eta$ of magnitude similar to values in $\mathbf{C}$, only the smaller differences in $\mathbf{C}$ would be negligible. Thereby, we can adjust the sparsity level of $\mathbf{w}$ by changing $\eta$. The sparsity path, i.e. elements of $\mathbf{w}_{S1}$ at different $\eta$, for an exemplar synthetic dataset (Section 3) is shown in Figure 1(a). At $\eta = 0$, corresponding to $\mathbf{w}_{S1}$ estimated using the original ORD formulation, only four out of eleven nodes in $S_1$ are correctly identified, which illustrates ORD's tendency to falsely split the subnetworks. As $\eta$ is increased, the true nodes (thicker red lines) gradually attain nonzero weights, i.e. become part of the identified subnetwork. However, choosing the optimal $\eta$ is non-trivial. Furthermore, noise in $\mathbf{C}$ could result in false nodes being included (thinner black lines). To jointly deal with these two problems, we propose integrating stability selection into the ORD formulation.

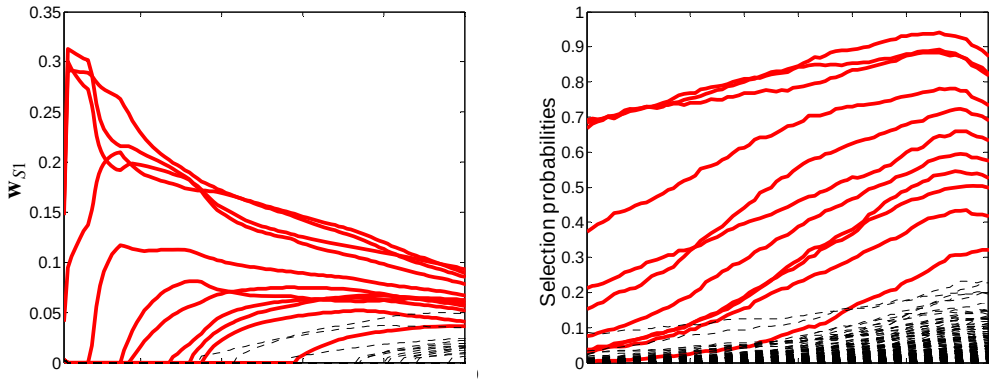


(a) Sparsity path (b) Stability path

Figure 1: Sparsity path vs. stability path for an exemplar synthetic dataset. Thicker red lines = nodes belonging to $S_1$. Thinner black lines = nodes not part of $S_1$. (a) ORD ($\eta = 0$) tends to falsely split the subnetwork, i.e. only 4/11 nodes in $S_1$ are correctly identified. By applying the graph incrementation scheme, more true nodes are correctly found as $\eta$ is increased, but false nodes are also included. Eventually, all nodes would be declared as a single subnetwork. (b) Instead of selecting a single specific $\eta$, stability selection operates by choosing a probability threshold that provably controls the expected number of false nodes in the identified subnetwork. If the selection probability for any $\eta$ exceeds the threshold, the associated nodes are declared as part of the subnetwork. For this example, all true nodes would be correctly identified if a threshold of 0.25 is used, with no false nodes included.

**Stability selection.** Given $\mathbf{C}$ and $\mathbf{w}_{S1}$, we generate a set of $\mathbf{C}_\eta$ by adding $\eta$ to the off-diagonal elements of $\mathbf{C}$ for a range of $\eta$ from $0.5 \cdot \max_{ij}|\mathbf{C}_{ij}|$ to $d \cdot \max_{ij}|\mathbf{C}_{ij}|$ at step size of $0.5 \cdot \max_{ij}|\mathbf{C}_{ij}|$, which typically adds ≤2 nodes at each $\eta$ increment. We then apply RD to each $\mathbf{C}_\eta$ with $\mathbf{w}(0)$ set to $\mathbf{w}_{S1} + 1/d$ (with elements renormalized to sum to 1) to avoid converging to a local maximum $\mathbf{w}_\eta$ that does not correspond to $\mathbf{w}_{S1}$. Adding $1/d$ is essential, since 0 in $\mathbf{w}(k)$ always remains as 0 as (2) is iterated, which prohibits new nodes to be added to $S_1$. $\mathbf{w}_\eta$ with more than $\theta = 10\%$ of its elements being non-zeros is discarded assuming a subnetwork would not span >10% of the brain. Increasing $\theta$ from 5% to 25%, ~$0.02d$ additional nodes are included, thus the estimated subnetworks are only mildly affected by the choice of $\theta$. Now, let $\mathbf{X}$ be a $t \times d$ time series matrix, where $t$ is the number of time samples. We generate 100 $\mathbf{X}^b$ by bootstrapping with replacement along the temporal dimension and compute $\mathbf{C}^b{}_\eta$ and $\mathbf{w}^b{}_\eta$. We highlight that it is important to set $\mathbf{w}^b{}_\eta(0)$ to $\mathbf{w}_{s1} + 1/d$ (normalized) to retain subnetwork correspondence across bootstrap samples. For each $\eta$ (including $\eta = 0$), we estimate the selection probability of each node as the proportion of bootstraps over which the corresponding element in $\mathbf{w}^b{}_\eta$ is non-zero. The stability path [12], i.e. selection probability of each node at different $\eta$, for the same synthetic dataset used in Figure 1(a) is shown in Figure 1(b). To identify nodes that belong to the same subnetwork, a threshold, $\tau$, that bounds the expected number of false nodes, $E$, is given by [12]:

$$E \leq \frac{1}{2\tau - 1} \frac{q^2}{d}, \tag{5}$$

where $q$ is the expected average number of nodes selected, which can be estimated as the sum of selection probability over nodes averaged across $\eta$. We set $E$ to 1 in deriving a $\tau$ that controls the expected number of false nodes per subnetwork to be ≤1. Given this $\tau$, we declare a node as part of subnetwork $S_1$ if its selection probability exceeds $\tau$ for any $\eta$ [12]. The same procedure is separately performed in refining each of the other subnetworks. The intuition behind stability selection is that the same false nodes are unlikely to be consistently selected over bootstrap samples. Importantly, stability selection is insensitive to the choice of $\eta$ [12]. Thus, integrating stability selection provides a statistically principled way for removing false nodes arising from noise and over-merging. For our data, which consist of time series from multiple subjects, we opt to bootstrap at the subject level.

## 3 Materials

**Synthetic data.** We generated 500 synthetic datasets that covers a wide range of network configurations to test the generality of SORD. Each dataset comprised $d = 200$ regions and 160 scans of 1200 time points as in the real data. The number of subnetworks, $N$, was randomly selected between 10 and 20 for each dataset. The number of regions in each subnetwork was set to $\lceil d/N \rceil + c$, where $c$ is a random integer between 1 and 5. The nodes in each subnetwork were randomly chosen from $\{1, \ldots, d\}$ and were allowed to repeat across subnetworks to generate subnetwork overlaps. For each configuration, a corresponding 200×200 adjacency matrix, $\mathbf{\Sigma}$, was created to generate ROI time courses by drawing samples from $N(0, \mathbf{\Sigma})$. Gaussian noise was added to the time courses with signal-to-noise ratio (SNR) randomly set between -6 and -10 dB. The noisy time courses across scans were temporally concatenated with their sample correlation matrix, $\mathbf{\Sigma}_s$, used as input to SORD.

**Real data.** Resting state fMRI (RS-fMRI) data from 40 subjects of the HCP database [15] were used. Each subject's dataset comprised two sessions, each having two scans of 15 min acquired with a TR of 0.72 s and a voxel size of 2 mm. Further details on acquisition can be found in [15]. In addition to the minimal preprocessing that was already performed on the HCP RS-fMRI data, which included gradient distortion correction, motion correction, spatial normalization, and intensity normalization, we further regressed out motion artifacts, white matter and cerebrospinal fluid confounds, and principal components of high variance voxels extracted using CompCor [18]. A bandpass filter at 0.01 to 0.1 Hz was subsequently applied. We functionally divided the brain into $d = 200$ ROIs by concatenating the preprocessed voxel time courses across scans of all subjects and applying Ward clustering [19]. ROI time courses were generated by averaging voxel time courses within each ROI, which were then concatenated across scans of all subjects for identifying subnetworks at the group level.

## 4 Results and Discussion

**Synthetic data.** We compared SORD against ORD [7], NC [3], and OSLOM [14] applied to $\mathbf{\Sigma}_s$ and temporal ICA (tICA) [6] applied to time courses drawn from $N(0, \mathbf{\Sigma})$. We chose NC and an ICA approach for comparisons since they are often used in fMRI studies, and OSLOM due to its superior performance over many state-of-the-art overlapping community detection techniques [14]. Note that we selected tICA over spatial ICA to enable more subnetwork overlaps [6]. Since NC and tICA do not have an intrinsic mechanism for setting the number of subnetworks, we used maximum modularity as the criterion [20]. To assess performance, we computed the mean Omega index [10], $\omega$, over the 500 synthetic datasets:

$$\omega = \frac{\omega_u - \omega_e}{1 - \omega_e}, \tag{6}$$

$$\omega_u = \frac{1}{d(d-1)/2} \sum_{n=0}^{\max(N_{\text{est}}, N_{\text{gnd}})} \left| t_n^{\text{est}} \cap t_n^{\text{gnd}} \right|, \tag{7}$$

$$\omega_e = \frac{1}{\left(d(d-1)/2\right)^2} \sum_{n=0}^{\max(N_{est}, N_{gnd})} \left| t_n^{est} \right| \cdot \left| t_n^{gnd} \right|, \tag{8}$$

where $N_{\text{est}}$ and $N_{\text{gnd}}$ are the estimated and ground truth number of subnetworks, respectively. $t_n^{\text{est}}$ is the set of node pairs that appear in exactly $n$ estimated subnetworks. $t_n^{\text{gnd}}$ is the counterpart for the ground truth subnetworks. $|\cdot|$ denotes cardinality. $\omega_u$ is the unadjusted Omega index and $\omega_e$ is the expected Omega index under the null, which is subtracted from $\omega_u$ to account for agreements in node pairs between the estimated and ground truth subnetworks that arise from chance alone. Overall, SORD achieved the best performance (Figure 2(a)). The pairwise $\omega$ differences between SORD and each contrasted method was statistically significant at $p = 10^{-10}$ based on the Wilcoxon signed rank test. $\omega$ of SORD was consistently ~0.02 greater than that of ORD for almost all synthetic datasets, hence the attained significance level. Our results thus show the robustness of SORD to various SNR and network configurations, comprising different subnetwork sizes and amount of overlaps.

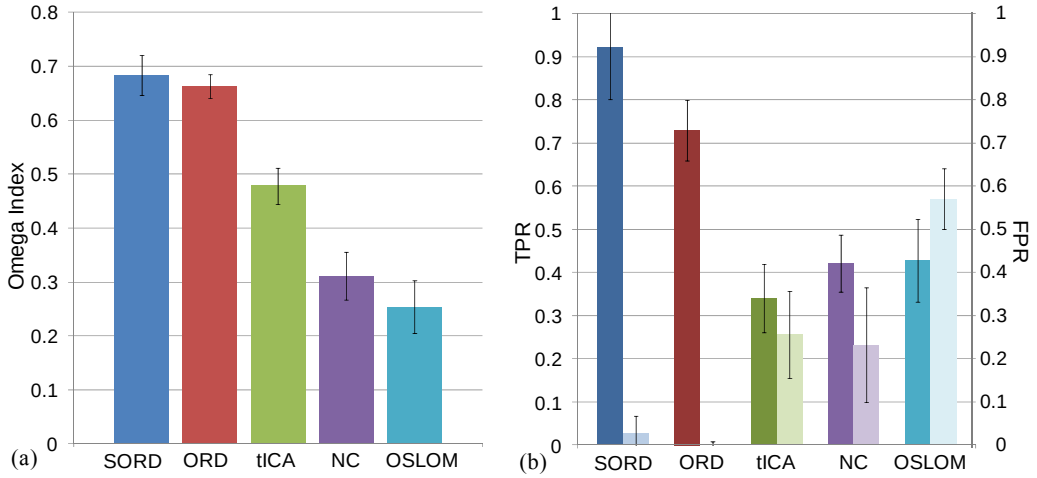


Figure 2: Subnetwork identification accuracy on synthetic data. (a) Omega index. (b) TPR = darker colour bars. FPR = lighter colour bars. Note FPR of ORD is ~0.001, not 0.

To more directly demonstrate that SORD alleviates the false subnetwork splitting problem in ORD, we computed the average true positive rate (TPR) and the average false positive rate (FPR) over the 500 synthetic datasets (Figure 2(b)):

$$\text{TPR} = \frac{1}{N_{gnd}} \sum_{l=1}^{N_{gnd}} \left| S_l^{est} \cap S_l^{gnd} \right| \Big/ \left| S_l^{gnd} \right|, \tag{9}$$

$$\mathrm{FPR} = \frac{1}{N_{gnd}} \sum_{l=1}^{N_{gnd}} \left| S_l^{est} \cap \bar{S}_l^{gnd} \right| \Big/ \left| \bar{S}_l^{gnd} \right|. \quad (10)$$

The estimated subnetwork $S_l^{\mathrm{est}}$ was matched to the ground truth subnetwork $S_l^{\mathrm{gnd}}$ using Hungarian clustering [21]. The TPR and FPR of the unmatched subnetworks were set to 0 and 1, respectively. SORD achieved the highest TPR among contrasted techniques with FPR well controlled. In particular, the increased TPR compared to ORD illustrates SORD's ability to merge the subnetwork components that were falsely split by ORD, while maintaining control over false node inclusion (0.44±0.62 nodes/subnetwork on average).

To evaluate the accuracy of the detected overlapping nodes, we computed the F-score = 2 · precision · recall / (precision + recall), where precision is the number of correctly detected overlapping nodes divided by the total number of detected overlapping nodes and recall is the number of correctly detected overlapping nodes divided by the true number of overlapping nodes [10]. The F-score of SORD (Figure 3(a)) was significantly higher than all contrasted techniques at $p = 10^{-10}$ based on the Wilcoxon signed rank test. In addition, for each detected overlapping node, we computed the proportion of subnetworks it was correctly assigned to, since the F-score does not account for how a detected overlapping node might e.g. be correctly assigned to only a portion of the ground truth subnetworks. The mean proportion over all detected overlapping nodes, i.e. $\mathrm{TPR_{ol}}$, and $\mathrm{FPR_{ol}}$ averaged over the 500 synthetic datasets are shown in Figure 3(b). SORD achieved the highest $\mathrm{TPR_{ol}}$ with $\mathrm{FPR_{ol}}$ well controlled. Note there is a misconception that the average correlation matrix contains no dynamical information [6]. It is true that the average correlation matrix does not capture dynamical connectivity, but the overlapping structure of subnetworks is well reflected by the relative magnitude of its elements, and can be readily extracted as shown by our results.

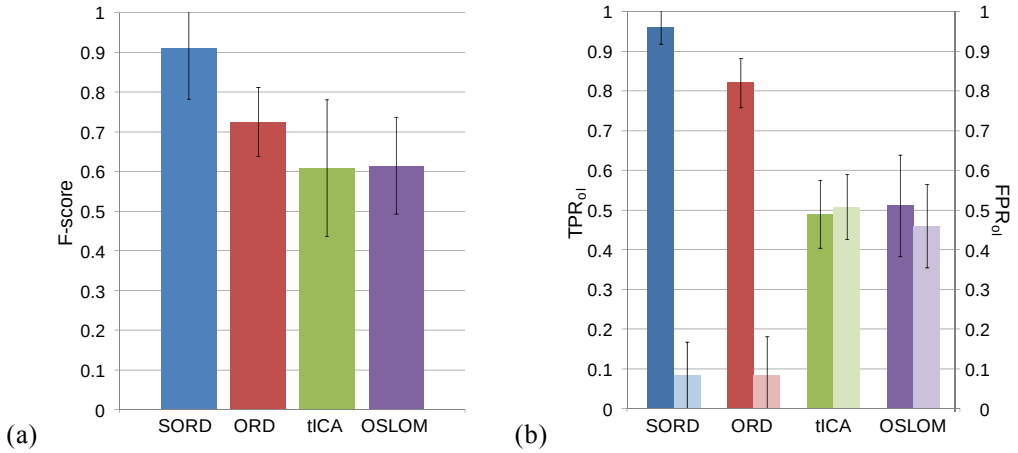


Figure 3: Overlapping node accuracy on synthetic data. (a) F-score. (b) $\mathrm{TPR_{ol}}$ = darker colour bars. $\mathrm{FPR_{ol}}$ = lighter colour bars.

**Real data.** To quantitatively evaluate the contrasted methods on real data, we used test-retest reliability as the metric. Specifically, we first extracted subnetworks separately from each of the two sessions of RS-fMRI data. We then computed the Omega index with subnetworks identified from first session's data taken as the "ground truth". The Omega index was 0.73 for SORD, 0.60 for ORD, 0.09 for ICA, 0.43 for NC, and 0.63 for OSLOM, which shows SORD's superior test-retest reliability, an attribute central for producing repeatable results.

Qualitatively, SORD found all the widely-observed networks reported in the literature [3], such as the default mode network, the executive control network (ECN), and the salience network, and additionally detected important subnetwork overlaps that would be neglected by graph partitioning methods, such as NC, and are seldom captured with spatial ICA [6]. For example, the salience network (Figure 4(a)) was found to overlap with the higher visual network, the auditory network, and the sensorimotor network, which provide further evidence for its role in deciphering salient sensory stimuli to guide behaviour [22].

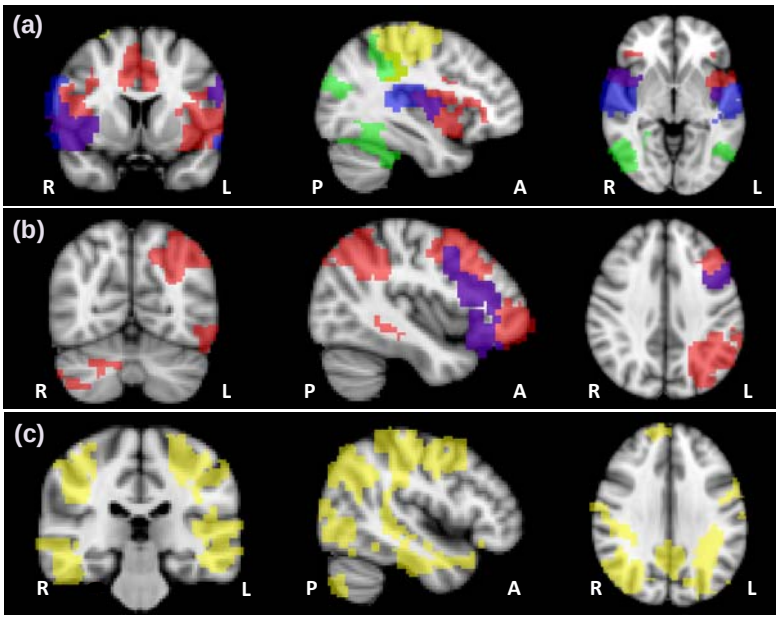


Figure 4: Exemplar subnetworks and hubs identified by SORD on real RS-fMRI data. L=left, R=right, A=anterior, P=posterior. Overlaps displayed as the mix of colors assigned to the subnetworks. (a) Salience network (red) was found to overlap with the higher visual network (green), the auditory network (blue), and the motor network (yellow) demonstrating its role in integrating processed sensory information for prioritizing attention [22]. (b) The executive control network extracted using ORD (blue) missed the parietal regions compared to SORD (red). (c) Hubs involved in three or more subnetworks.

Comparing SORD and ORD (Figure 4(b)), ORD was found to over-divide the known networks, e.g. the parietal regions were missing in the ECN [22]. Examining the overlaps across subnetworks identified by SORD, prominent hubs (Figure 4(c)) were found within the superior/inferior parietal cortex, superior/middle/inferior temporal cortex, medial superior frontal cortex, lateral occipital cortex, posterior cingulate gyrus, and precuneous, which match well with brain regions previously reported [23]. To characterize these hubs, we computed their betweenness centrality [23]. Hubs involved in $\geq 3$ subnetworks constitute 17% of the total number of brain regions, and the difference between their betweenness centrality and the rest of the brain is significant at $p = 0.001$ based on the Wilcoxon rank sum test, thus confirming the detected subnetwork overlaps are not artificial.

## 5 Conclusions

We proposed SORD for identifying overlapping subnetworks from weighted graphs with statistical control over false node inclusion. By exploiting a graph incrementation scheme and incorporating stability selection, the subnetwork splitting problem inherent in ORD is alleviated. On a wide variety of simulated network configurations, SORD was shown to outperform a number of state-of-the-art techniques, including ORD, NC, temporal ICA, and OSLOM. Higher test-retest reliability was also obtained on real data, which demonstrates SORD's greater robustness to inter-session variability, an important attribute that is receiving growing attention from the neuroimaging community.

## References

[1] Li, K., Guo, L., Nie, J., Li, G. & Liu, T. (2009) Review of methods for functional brain connectivity detection using fMRI. *Computerized Medical Imaging and Graphics* **33**(2):131-139.

[2] Labatut, V. & Balasque, J.-M. (2012) Detection and interpretation of communities in complex networks: Practical methods and application. In A. Abraham and A.-E. Hassanien (eds.), *Computational Social Networks*, pp. 81-113. London: Springer-Verlag.

[3] Van Den Heuvel, M., Mandl, R. & Hulshoff Pol, H. (2008) Normalized cut group clustering of resting-state fMRI data. *PLoS ONE* **3**(4):e2001.

[4] Wu, K., Taki, Y., Sato, K., Sassa, Y., Inoue, K., Goto, R., Okada, K., Kawashima, R., He, Y., Evans, A.C. & Fukuda, H. (2011) The overlapping community structure of structural brain network in young healthy individuals. *PLoS ONE* **6**(5):e19608.

[5] Yan, X., Kelley, S., Goldberg, M. & Biswal, B.B. (2011) Detecting overlapped functional clusters in resting state fMRI with connected iterative scan: A graph theory based clustering algorithm. *Journal of Neuroscience Methods* **199**(1):108-118.

[6] Smith, S.M., Miller, K.L., Moeller, S., Xu, J., Auerbach, E.J., Woolrich, M.W., Beckmann, C.F., Jenkinson, M., Andersson, J., Glasser, M.F., Van Essen, D.C., Feinberg, D.A., Yacoub, E.S. & Ugurbil, K. (2012) Temporally-independent functional modes of spontaneous brain activity. *Proceedings of the National Academy of Sciences* **109**(8):3131-3136.

[7] Yoldemir, B., Ng, B. & Abugharbieh, R. (2013) Overlapping replicator dynamics for functional subnetwork identification. In K. Mori, I. Sakuma, Y. Sato, C. Barillot, N. Navab, N. (eds.), *Medical Image Computing and Computer Assisted Intervention*, LNCS 8150, pp. 682-689. Berlin Heidelberg: Springer-Verlag.

[8] Ng, B., Abugharbieh, R. & McKeown, M.J. (2012) Group replicator dynamics: A novel group-wise evolutionary approach for sparse brain network detection. *IEEE Transactions on Medical Imaging* **31**(3):576-585.

[9] Thirion, B., Pinel, P., Tucholka, A., Roche, A., Ciuciu, P., Mangin, J.-F. & Poline, J.-B. (2007) Structural analysis of fMRI data revisited: Improving the sensitivity and reliability of fMRI group studies. *IEEE Transactions on Medical Imaging* **26**(9):1256-1269.

[10] Xie, J., Kelley, S. & Szymanski, B.K. (2013) Overlapping community detection in networks: The state-of-the-art and comparative study. *ACM Computing Surveys* **45**(4):43:1-43:35.

[11] Van de Geer, S., Bühlmann, P. & Ritov, Y. (2013) On asymptotically optimal confidence regions and tests for high-dimensional models. arXiv preprint, arXiv:1303.0518.

[12] Meinshausen, N. & Bühlmann, P. (2010) Stability selection. *Journal of the Royal Statistical Society: Series B (Statistical Methodology)* **72**(4):417-473.

[13] Lockhart, R., Taylor, J., Tibshirani, R.J. & Tibshirani, R. (2014) A significance test for the lasso. *Annals of Statistics* **42**(2):413-468.

[14] Lancichinetti, A., Radicchi, F., Ramasco, J.J. & Fortunato, S. (2011) Finding statistically significant communities in networks. *PLoS ONE* **6**(4):e18961.

[15] Van Essen, D.C., Smith, S.M., Barch, D.M., Behrens, T.E.J., Yacoub, E. & Ugurbil, K. (2013) The WU-Minn Human Connectome Project: An overview. *NeuroImage* **80**:62-79.

[16] Schuster, P. & Sigmund, K. (1983) Replicator dynamics. *Journal of Theoretical Biology* **100**:533-538.

[17] Torsello, A., Bulo, S.R. & Pelillo, M. (2008) Beyond partitions: Allowing overlapping groups in pairwise clustering. In *IEEE International Conference on Pattern Recognition*, pp. 1-4.

[18] Behzadi, Y., Restom, K., Liau, J. & Liu, T.T. (2007) A component based noise correction method (CompCor) for BOLD and perfusion based fMRI. *NeuroImage* **37**(1):90-101.

[19] Michel, V., Gramfort, A., Varoquaux, G., Eger, E., Keribin, C. & Thirion, B. (2012) A supervised clustering approach for fMRI-based inference of brain states. *Pattern Recognition* **45**(6):2041-2049.

[20] Wang, Q. & Fleury, E. (2012) Fuzziness and overlapping communities in large-scale networks. *Journal of Universal Computer Science* **18**(3):457-486.

[21] Kuhn, H.W. (1955) The Hungarian method for the assignment problem. *Naval Research Logistics Quarterly* 2:83-97.

[22] Seeley, W.W., Menon, V., Schatzber, A.F., Keller, J., Glover, G.H., Kenna, H., Reiss, A.L. & Greicius, M.D. (2007) Dissociable intrinsic connectivity networks for salience processing and executive control. *The Journal of Neuroscience* **27**(9):2349-2356.

[23] Buckner, R.L., Sepulcre, J., Talukdar, T., Krienen, F.M., Liu, H., Hedden, T., Andrews-Hanna, J.R., Sperling, R.A. & Johnson, K.A. (2009) Cortical hubs revealed by intrinsic functional connectivity: Mapping, assessment of stability, and relation to Alzheimer's disease. *The Journal of Neuroscience* **29**(6):1860-1873.